Neoplasma 2023; 70(4): 534–544

doi:10.4149/neo_2023_230307N121

Migration-inducing gene-7 promotes glioma cell proliferation and invasiveness via activating the MAPK signaling pathway

Zhigang PAN, Chunhui CHEN, Xinyue HUANG, Yu XIONG, Xiaodong KANG, Jianfeng ZHOU, Xiumei GUO, Shuni ZHENG*, Cui'e WANG*, Feng ZHENG*, Weipeng HU*

Department of Neurosurgery, The Second Affiliated Hospital, Fujian Medical University, Quanzhou, Fujian, China

**Correspondence: hwp1984@fjmu.edu.cn; dr.feng.zheng@gmail.com; 1287438611@qq.com; 303515771@163.com*

Received March 7, 2023 / Accepted August 8, 2023

Glioma is a highly aggressive primary malignant tumor. Migration-inducing gene-7 (Mig-7) is closely related to tumor invasion and metastasis. However, the detailed molecular mechanism of Mig-7-mediated promotion of glioma cell invasion requires further investigation. Therefore, this study aimed to investigate the molecular mechanism by which Mig-7 promotes invasion and growth of glioma tumor cells. After collecting 65 glioma tissues and 16 non-tumor tissues, the expression difference of Mig-7 between tumor tissues and non-tumor tissues was analyzed. The molecular mechanism of Mig-7 in tumor cells was investigated by knockdown or overexpression of Mig-7 in U87MG cells. Specifically, the expression levels of mitogen-activated protein kinase (MAPK) signaling pathway-related molecules were detected in cells that knocked down Mig-7. MTT, Transwell, and three-dimensional cell culture assays were used to detect the survival, migration, invasion, and tube formation of U87MG cells that overexpressed Mig-7 were treated with the MAPK signaling pathway inhibitors (SP600125, SCH772984, and SB202190). The effect of Mig-7 on the tumorigenic ability of U87MG cells was investigated by subcutaneous tumorigenic experiment in nude mice. The corresponding results indicated that Mig-7 expression was significantly higher in glioma tissues and cell lines compared to that in non-neoplastic brain tissues and normal glial cell lines. In U87MG cells, downregulation or overexpression of Mig-7 inhibited or promoted the expression of MMP-2, MMP-9, LAMC2, EphA2, and VE-cadherin, and phosphorylation levels of ERK1/2, JNK, and p38. Mig-7 overexpression promoted migration, invasion, cell viability, and tube formation, which were reversed by the MAPK signaling pathway inhibitors. Mig-7 overexpression promoted subcutaneous tumor growth in mice and upregulated the phosphorylation levels of ERK1/2, JNK, and p38 and the expression of Ki-67. These effects of Mig-7 overexpression were reversed by MAPK pathway inhibitors. Overall, these results suggest that Mig-7 may be a novel biomarker and potential therapeutic target for glioma, with the MAPK pathway playing a key role in the corresponding Mig-7 mechanism of action.

Key words: glioma; migration-inducing gene-7; MAPK signaling pathway; invasion

Glioma is the most aggressive primary brain tumor, with surgical resection, radiotherapy, and chemotherapy as potential treatment options. However, the 5-year survival rate of glioma patients is less than 10%, and the corresponding recurrence and mortality rates remain high [1–3]. Therefore, it is necessary to further understand the molecular mechanisms underlying glioma occurrence and progression to facilitate the development of more effective novel drugs.

Migration-inducing gene-7 (Mig-7) protein is composed of 207 amino acids and is rich in cysteine [4]. It has been revealed that Mig-7 mRNA levels increase in embryonic cytotrophoblast cells and in more than 80% of tumors [4–6]. Recently, Mig-7-specific shRNA and anti-Mig-7 (1e9) polyclonal antibodies were produced; it was reported that targeting Mig-7 protein with these inhibitory mechanisms reduced HEC1A endometrial carcinoma cell chemoinvasion and MT1-MMP activation [7]. Mig-7 significantly affects tumor migration and invasion in hepatocellular carcinoma and osteosarcoma, while it is essential for proliferation and invasion in ovarian cancer [8, 9]. Further, Mig-7 is overexpressed in highly invasive tumors but not in non-invasive malignant cells [10–13], suggesting an important role in tumor invasion. Additionally, knocking down Mig-7 attenuates the invasiveness of U87MG cells [12]. However, it remains to be investigated whether Mig-7 affects the proliferation of glioma cells [12].

Previous studies have shown that excessive proliferation, migration, and invasion of glioma cells are associ-

ated with the activation of various oncogenic cascades [14]; among these cascades, the mitogen-activated protein kinase (MAPK) pathway is aberrantly activated in gliomas and is associated with the resultant proliferation, migration, and invasion [15, 16]. Three typical subfamilies of MAPKs exist: ERKs, JNKs, and p38s [16]. The MAPK signaling pathway is a promising target for tumor therapy; therefore, it is important to discover novel anti-cancer targets by analyzing this pathway [17]. Our previous study demonstrated that the PI3K/AKT/MMP pathway plays an important role in Mig-7-dependent regulation of glioma invasiveness, including via the mediation of MMP-2 and MMP-9 [12]. MMP-2 promotes LAMC2 cleavage, which promotes cytoskeletal recombination and movement by activating downstream targets of the epidermal growth factor receptor; further, studies have shown that the expression of MMP-2 and MMP-9 in glioma can be suppressed by inhibiting MAPK pathway [8]. In addition, Mig-7 regulates ERK and AKT phosphorylation levels in endometrial carcinoma and, ultimately, affects tumor growth [7]. However, it has not been reported whether Mig-7 can affect the growth of glioma tumors by regulating ERK, JNKs, and p38 pathways.

Therefore, the aim of this study was to examine the expression of Mig-7 in glioma tissues and cell lines in comparison to non-tumorigenic tissues and normal glial cell lines, alongside elucidating the role of the MAPK pathway in Mig-7-mediated regulation of glioma cell migration, invasion, cell viability, and tube formation.

Patients and methods

Cell lines and tissue samples. HA1800, LN-229, U87MG, and Hs 683 cell lines were purchased from the cell bank of the Chinese Academy of Sciences (Shanghai, China). All cells were cultured at 37 °C under 5% CO_2 in Dulbecco's modified Eagle medium (DMEM, catalog number: 11965092, Gibco, USA) supplemented with 10% fetal bovine serum (FBS, catalog number: 10099141C, Gibco, Australia), penicillin-streptomycin (penicillin: 100 U/ml, streptomycin: 100 µg/ml, catalog number: 15140148, Gibco, USA). The tissue sample collection and analysis used in this study were approved by the Ethics Committee of the Second Affiliated Hospital of Fujian Medical University (Ethics approval number: No.262 [2021]). In addition, 65 glioma tissues and 16 non-tumor tissues were collected from the Pathology Department of the Second Affiliated Hospital of Fujian Medical University from 2019 to 2021, including 6 pairs of glioma tissue and adjacent normal tissue.

Immunohistochemistry (IHC). Immunohistochemical staining was performed as previously described [18]. Briefly, paraffin-embedded tissue samples were cut into 5 µm thick sections using a microtome (HistoCore BIOCUT, Leica Biosystems, Germany). The sections were blocked with 5% goat serum for 15 min at 26 °C and incubated overnight with mouse anti-Mig-7 (1:500, catalog number: ab272576, Abcam Co. Ltd, Cambridge, UK) or rabbit anti-Ki-67 (1:2000, catalog number: 27309-1-AP, Proteintech, Wuhan, China) at 4 °C. After washing with phosphate-buffered saline (PBS), the sections were incubated with horseradish peroxidase (HRP)-conjugated goat anti-mouse IgG (catalog number: SA00001-1, Proteintech, China) or anti-rabbit IgG (catalog number: SA00001-2, Proteintech, China) for 20 min at 25 °C. The sections were washed once more with PBS and the colorimetric reaction was developed by diaminobenzidine (catalog number: P0203, Beyotime, Shanghai, China). After counterstaining with hematoxylin (catalog number: ST2067-5g, Beyotime, China) and dehydration, the sections were observed and photographed under an optical microscope (Olympus, Japan) in a bright field (100× or 200× magnification). The percentage of Ki-67-positive cells was estimated under a microscope, 1,000 tumor cells were counted randomly, and the Ki-67-positive rate was calculated (number of positive cells/1000×100%; n=6/group).

RNA extraction and real-time PCR. Total RNA was extracted from the tissues and cells using TRIzol (catalog number: 15596026CN, Invitrogen, USA) according to the manufacturer's instructions. The absorption value of RNA solution at 260 nm was measured by ultra microspectrophotometer (Implen, model: Nanophotometer NP80, Germany), and the quality and concentration of RNA were analyzed. cDNA was synthesized using the obtained RNA and reverse transcription kit (catalog number: RR036A, TaKaRa, Osaka, Japan) according to the manufacturer's instructions. Real-time PCR was performed on a MiniOpticon Real-Time PCR detection system (Bio-Rad, USA) with the GoTaq® qPCR Master Mix (catalog number: A6001, Promega, WI, USA) using the obtained cDNA. The relevant primers designed by using DNAMAN software (version 9.0) are listed in Table 1. Real-time PCR conditions were as follows: initial denaturation at 95 °C for 2 min, followed by 40 cycles of denaturation for 15 s at 95 °C and annealing/elongation for 60 s at 60 °C. 18S RNA was used for the internal control for normalization. These results were calculated with the $2^{-\Delta\Delta Ct}$ method [19]. All samples were run in triplicates.

Western blotting. Total protein from the tissues and cells was extracted with RIPA lysis buffer (catalog number: 89900, Thermo Fisher Scientific, Waltham, MA, USA) containing phenylmethylsulfonyl fluoride (catalog number: ST505, Beyotime, China) and phosphorylated protease inhibitors (catalog number: G2007-1ML, Servicebio, China), and quantified with a bicinchoninic acid kit (catalog number: 23250, Thermo Fisher Scientific, China). Next, the proteins separated in a 10% sodium dodecyl sulfate-polyacrylamide gel electrophoresis were transferred to the PVDF membranes (catalog number: IPVH00010, Millipore, USA) in ice water for 90 min. During electrophoresis, the initial voltage was 80 V, and when the sample ran to the separation gel, the voltage was increased to 120 V until the end of electrophoresis. During membrane transfer, the current was 240 mA for 1 h. Next, the membranes were blocked with 5% non-fat milk and incubated overnight with primary antibodies against

Mig-7 (1:2000, catalog number: bs-5781R, Bioss Antibodies, Beijing, China), EphA2 (1:2000, catalog number: 66736-1-Ig, Proteintech, China), LAMC2 (1:3000, catalog number: 19698-1-AP, Proteintech, China), VE-cadherin (1:2000, catalog number: 66804-1-Ig, Proteintech), MMP-2 (1:2000, catalog number: 10373-2-AP, Proteintech), MMP-9 (1:3000, catalog number: 10375-2-AP, Proteintech), phospho-ERK (1:1000, catalog number: 4376S, Cell Signaling Technology, USA), ERK (1:1000, catalog number: 4695S, Cell Signaling Technology), phospho-JNK (1:1000, catalog number: 9255S, Cell Signaling Technology, JNK (1:1000, catalog number: 9252S, Cell Signaling Technology), phospho-p38 (1:1000, catalog number: 9216S, Cell Signaling Technology), p38 (1:1000, catalog number: 9212S, Cell Signaling Technology) and GAPDH (1:1000, catalog number: 2118S, Cell Signaling Technology) at 4 °C. The membranes were then incubated with HRP-labeled goat anti-mouse IgG (catalog number: SA00001-1, Proteintech) or anti-rabbit IgG (catalog number: SA00001-2, Proteintech) at room temperature for 2 h. The immunoblots were visualized with the ECL Western Blotting Detection System (Forevergen, China). ImageJ was used to analyze the optical densities of the target bands. The target protein expression levels were normalized using GAPDH as an internal control.

Overexpression or knockdown of Mig-7 in U87MG cells. For Mig-7 silencing, we designed small interfering RNA (siRNA) targeting Mig-7 (si-Mig-7) and the negative control of si-Mig-7 (si-NC) using the software of Ambion siRNA Target Finder (Ambion, Inc., USA); these were then synthesized by GenePharma Company (Shanghai, China). U87MG cells were seeded into 6-well plates at a density of 5×10^5 cells/well. When the cell confluence reached 60%, siRNA (si-Mig-7 or si-NC) was transfected into the cells at 100 pmol/well using Lipofectamine® 2000. Mig-7 silencing was verified by real-time PCR and western blotting. The sequences of siRNA are listed in Table 2.

For the stable overexpression of Mig-7, Mig-7 (GeneBank: DQ080207.2) was inserted into the pcDNA3.3-puro vector (XIAMEN Anti-HeLa Biological Technology Trade Co., Ltd., Xiamen, China) to prepare the lentiviruses. The resulting plasmid was named Mig-7 OE. The corresponding primer sequences were designed and synthesized (Table 2).

To prepare the lentiviral particles, 9 μg of Mig-7 OE and the suitable packaging plasmids (3 μg of pMD2G and 6 μg of pspax2) were co-transfected into 293T cells (Xiamen Immocell Biotechnology Co., Ltd.) using Lipofectamine® 2000 (Invitrogen; Thermo Fisher Scientific, Inc.). After 48 h, the supernatant, which contained the lentivirus, was collected, and then the lentivirus was enriched and the titer was determined as described previously [20]. In the presence of 8 μg/ml polypropylene, the lentivirus was transduced into U87MG cells at a multiplicity of infection of 10. After 48 h, the medium was replaced with fresh medium, and puromycin was added at a final concentration of 600 ng/ml. After 14 days, cells were collected for Mig-7 expression analysis.

Inhibitor treatment. 10 μM JNKs inhibitor SP600125 (catalog number: S1460, Selleck, USA) [21], 2 μM ERK inhibitor SCH772984 (catalog number: S7101, Selleck) [22], or 10 μM p38 inhibitor SB202190 (catalog number: S1077, Selleck) [23] were used to treat with U87MG cells stably overexpressing Mig-7 for 24 h. For cell treatments, the drug is dissolved in dimethyl sulfoxide (DMSO, catalog number: ST038, Beyotime, China) and then diluted in the medium immediately prior to use. The final concentration of DMSO was less than 0.1%.

Cell viability assay. U87MG cells with stable overexpression of Mig-7 and the corresponding control cells were seeded in a 96-well plate at a density of 5×10^3 cells/well for

Table 1. The relevant sequence-specific primers used in real-time PCR.

Gene	Forward primer (5′-3′)	Reverse primer (5′-3′)
EphA2	ACTGCCAGTGTCAGCATCAACC	GTGACCTCGTACTTCCACACTC
LAMC2	TACAGAGCTGGAAGGCAGGAT	GTTCTCTTGGCTCCTCACCTTG
Mig-7	TGCCAAGTCTGGAATAGTCCTAGT	CTCTCCTCGGTCTGTCTTCTTGA
MMP-2	AGCGAGTGGATGCCGCCTTTAA	CATTCCAGGCATCTGCGATGAG
MMP-9	CATTCCAGGCATCTGCGATGAG	CCCTCAGAGAATCGCCAGTAC
VE-cadherin	CGCAATAGACAAGGACAT	GCCGTGTTATCGTGATTA
GAPDH	GAGTCAACGGATTTGGTCGT	GACAAGCTTCCCGTTCTCAG

Table 2. Sequence of siRNA and primers for plasmid construction.

Name	Sequence (5′-3′)
si-NC	TTCTCCGAACGTGTCACGT
si-Mig-7-1	CGTGTGTGTGTGTGTGTGTGT
si-Mig-7-2	CGCTAGACAAAGTCAAGAAGAC
si-Mig-7-3	CGTTGAAAGTGTAGCTGCATC
Mig-7 OE forward primer	TAGAGAATTCGGATCCGCCACCATGGCAGCAAGTAGATGCTC
Mig-7 OE reverse primer	GCTTCCATGGCTCGAGTTACAGTTTAAATGTGAACACTTTTGC

4 h. After cells were treated with SP600125, SCH772984, or SB202190 for 24 h, 20 µl 3-(4,5-dimethylthiazol-2-yl)-2,5-diphenyltetrazolium bromide (MTT, 5 mg/ml, catalog number: ST316, Beyotime, China) solution was added. After incubation for 4 h at 37 °C, the supernatant was discarded and DMSO was added to each well. The plates were gently shaken on a horizontal shaker for 10 min to dissolve crystals. The optical density value of each well was read at 490 nm in a microplate reader (BioTek, USA). The experiment was repeated thrice.

Cell migration and invasion assays. For migration or invasion assays, U87MG cells with stable overexpression of Mig-7 and the corresponding control cells in 100 µl DMEM (without FBS) containing SP600125, SCH772984, or SB202190 were seeded in the Matrigel-free or Matrigel-coated upper chambers of the 24-well Transwell plates (Corning, USA) at a density of 1×10^5 cells/well, and 500 µl DMEM with 10% FBS was plated in the lower chambers of the Transwell plates. After 24 h of incubation at 37 °C, the cells at the back of the upper chamber bottom were fixed in 4% paraformaldehyde (catalog number: P0099, Beyotime, China) for 30 min and stained in 0.5% crystal violet (catalog number: C0121, Beyotime) for 30 min. Cells were photographed under an optical microscope in a bright field (100× magnification) and counted using ImageJ software.

Three-dimensional cell culture. Matrigel (Becton, Dickinson and Company, New Jersey, USA) and FBS (Gibco Inc.) were mixed at a 1:1 ratio, and then 20 µl of this mixture was immediately added to each well of the 24-well plate and evenly spread on the bottom. After the gel was coagulated, 1×10^5 U87MG cells with stable overexpression of Mig-7 and the corresponding control cells in 100 µl DMEM with SP600125, SCH772984, or SB202190 were added to each well. After 6 h, the cells were viewed and photographed with a light microscope in a bright field (40× magnification). ImageJ software was used to calculate the formation of tubes.

Tumor formation assay *in vivo*. All animal experiments took place at the Second Affiliated Hospital of Fujian Medical University and were approved by the Second Affiliated Hospital of Fujian Medical University Institutional Ethics Committee (No.262 [2021]). Four-week-old male BALB/c athymic nude mice were purchased from the National Laboratory Animal Center (Beijing, China), and maintained under specific pathogen-free (SPF) conditions for a week before the experiment began. Six mice were placed in a cage. Eighteen mice were divided into three groups with 6 mice in each group: overexpressing negative control (Ctrl), overexpressing Mig-7 (Mig-7 OE), and Mig-7 OE+MAPK inhibitor group, with 6 mice in each group. In the Ctrl group, control cells were injected subcutaneously into mice with 5×10^6 cells/mouse; then 200 µl normal saline was injected intraperitoneally every day. In Mig-7 OE group, U87MG cells overexpressing Mig-7 were injected subcutaneously into mice with 5×10^6 cells/mouse; then 200 µl normal saline was injected intraperitoneally every day. In the Mig-7 OE+MAPK inhibitor group, U87MG cells overexpressing Mig-7 were subcutaneously injected into mice with 5×10^6 cells/mouse; then intraperitoneally injected with 30 mg/kg SP600125 [24], 25 mg/kg SCH772984 [25], and 5 mg/kg SB202190 [26] every day. The drug is dissolved in DMSO and then diluted in the PBS immediately prior to use. These drugs were then injected intraperitoneally daily. Tumor growth was measured at 0, 20, 24, 28, 32, 36, and 40 days after cell injection, and the tumor volume was calculated using the formula: volume (mm^3) = 0.5 × length × width × width. After 40 days of the subcutaneous injection, all mice were placed in the euthanasia chamber and then euthanized by introducing 100% CO_2 gas at a flow rate of 60% of the chamber volume/min. The mice were confirmed dead when there was no corneal reflex, detectable breathing, and heartbeat for more than 5 min. After being euthanized, the tumor tissues from the mice were resected, imaged, weighed, and either snap frozen in liquid nitrogen or embedded in paraffin for IHC.

Statistical analyses. Statistical analyses were performed using SPSS 17.0 software. All experiments were independently performed three times. Data normality was assessed using the Kolmogorov-Smirnov and Shapiro-Wilk tests, and homogeneity of variances was assessed using the Levene test. All studied variables did not deviate from normal distribution and variances did not significantly differ between conditions for the same variable. Two groups were compared using an unpaired or paired Student's t-test. Multiple groups were compared by one-way ANOVA, followed by the Tukey's post hoc test. Categorical data were compared using the Chi-square test. Data was considered with statistical significance with $p<0.05$. Data are expressed as mean ± standard deviation.

Results

Mig-7 is upregulated in glioma tissues and glioma cell lines. Positive expression of the Mig-7 protein in glioma and non-neoplastic brain tissues was found in 59 (90.7%) and 2 (12.5%) cases, respectively; in contrast, negative expression of the Mig-7 was found in 6 (9.3%) and 14 (87.5%) samples, respectively. Thus, Mig-7 was significantly upregulated in glioma tissues compared to non-tumorigenic brain tissues (categorical data, chi-square test 42.3, $p<0.0001$, Table 3). Moreover, IHC and western blot showed that Mig-7 protein levels were higher in glioma tissues than in non-tumorigenic brain tissues (Figures 1A–1C; paired two groups, paired

Table 3. Different protein expression of Mig-7 between glioma and non-neoplastic brain tissues.

Group	Cases	Mig-7 protein expression		χ^2	p-value
		No. of negative n (%)	No. of positive n (%)		
Glioma tissues	65	6	59	42.3	<0.0001
Non-neoplastic tissues	16	14	2		

Student's t-test, t=2.586, p=0.0491, Figure 1C). Similarly, Mig-7 mRNA levels were higher in glioma tissues than those in non-tumorigenic brain tissues (paired two groups, paired Student's t-test, t=3.077, p=0.0276, Figure 1D).

In vitro glioma cell models, including the LN229, U87MG, and Hs 683 cell lines, were used to assess Mig-7 expression. The corresponding results demonstrated that Mig-7 mRNA and protein expression were significantly higher in glioma cell lines than those in the normal glial cell line HA1800 (Figures 1E–1G) (multiple groups, one-way ANOVA, Figure 1E, $F_{3,8}$=478.7, p<0.0001; Figure 1G, $F_{3,8}$=118.3, p<0.0001).

Knockdown of Mig-7 decreases the expression levels of extracellular matrix-related molecules, and phosphorylation levels of ERK1/2, JNK, and p38. To explore the inhibition of extracellular matrix-related molecules and MAPK pathway expression after Mig-7 silencing, U87MG cells were transfected with si-Mig-7. The expression of Mig-7 mRNA and protein levels were dramatically reduced in the si-Mig-7 group compared with the non-transfected (mock) group and si-NC group cells; this confirmed that Mig-7 was inhibited by si-Mig-7 (Figures 2A–2C) (multiple groups, one-way ANOVA; Figure 2A, Mig-7: $F_{2,6}$=628.4, p<0.0001; Figure 2C, Mig-7: $F_{2,6}$=1205, p<0.0001). After decreasing Mig-7 expression, MMP-2, MMP-9, LAMC2, EphA2, and VE-cadherin mRNA and protein levels were found to be significantly lower in the si-Mig-7 group than those in the si-NC group (Figures 2A–2C) (multiple groups, one-way ANOVA; Figure 2A, MMP-2: $F_{2,6}$=155.1, p<0.0001, MMP-9: $F_{2,6}$=232.4, p<0.0001, LAMC2: $F_{2,6}$=36.68, p=0.0004, EphA2: $F_{2,6}$=45.31, p=0.0002, VE-cadherin: $F_{2,6}$=126.8, p<0.0001; Figure 2C, MMP-2: $F_{2,6}$=56.27, p=0.0001, MMP-9: $F_{2,6}$=424.8, p<0.0001, LAMC2: $F_{2,6}$=858.6, p<0.0001, EphA2: $F_{2,6}$=166.5, p<0.0001, VE-cadherin: $F_{2,6}$=140.4, p<0.0001). These findings suggest that Mig-7 has the potential to regulate extracellular matrix formation.

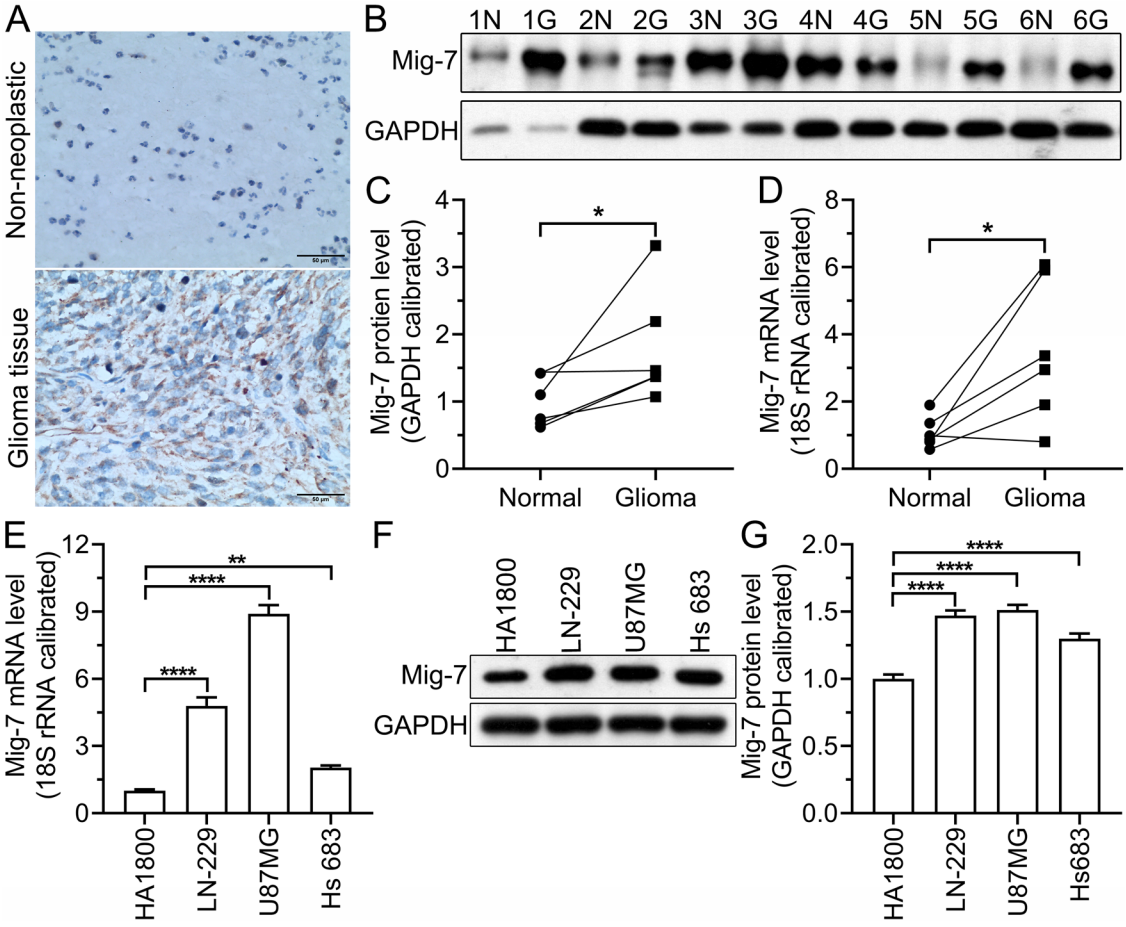

Figure 1. Mig-7 is upregulated in glioma tissues and glioma cell lines. A) Representative IHC images show Mig-7 expression levels in non-neoplastic (n=6) and glioma tissues (200× magnification, n=6). B–D) The protein (B, C) and mRNA (D) levels of Mig-7 in glioma (n=6) and paired non-neoplastic brain tissues (n=6). E–G) The mRNA (E) and protein (F, G) levels of Mig-7 in HA1800, LN229, U87MG, and Hs 683 cell lines. The experiment was carried out independently three times (n=3). Paired Student's t-test was applied to analyze differences between two groups in C and D. One-way ANOVA was applied for statistical analysis in E and F. *p<0.05, **p<0.01, ****p<0.0001. Abbreviation: Mig-7- migration-inducing gene-7

In addition, the protein expression levels of phospho-ERK, phospho-JNK, and phospho-p38 protein expressions were significantly downregulated in the si-Mig-7 group relative to the mock and si-NC group (Figures 2B, 2C) (multiple groups, one-way ANOVA, Figure 2C; phospho-ERK1/2/ERK1/2: $F_{2,6}$=13.23, p=0.0063, phospho-JNK/JNK: $F_{2,6}$=13.02, p=0.0066, phospho-p38/p38: $F_{2,6}$=31.61, p=0.0007). Overall, these results showed that the MAPK signaling pathway was inhibited by silencing Mig-7.

Mig-7 strengthens the expression levels of extracellular matrix-related molecules by activating the MAPK signaling pathway. To investigate whether Mig-7 regulates the expression of extracellular matrix-related molecules by activating the MAPK signaling pathway, we used MAPK signaling pathway inhibitors (SP600125, SCH772984, or SB202190) to treat Mig-7-overexpressing U87MG cells. Upregulation of Mig-7 increased the expression of MMP-2, MMP-9, LAMC2, EphA2, and VE-cadherin and levels of phospho-JNK, phospho-ERK, phospho-p38, whereas the use of MAPK signaling pathway inhibitors mitigated these Mig-7-mediated effects (Figures 3A, 3B) (multiple groups, one-way ANOVA; Figure 3B, Mig-7: $F_{5,12}$=152.8, p<0.0001, phospho-p38/p38: $F_{5,12}$=324.1, p<0.0001, phospho-ERK/ERK: $F_{5,12}$=47.44, p<0.0001, phospho-JNK/JNK: $F_{5,12}$=406.5, p<0.0001, MMP-2: $F_{5,12}$=255.4, p<0.0001, MMP-9: $F_{5,12}$=191.5, p<0.0001, LAMC2: $F_{5,12}$=36.65, p<0.0001, EphA2: $F_{5,12}$=75.18, p<0.0001, VE-cadherin: $F_{5,12}$=110.0, p<0.0001). Overall, Mig-7 regulates the expression of MMP-2, MMP-9, LAMC2, EphA2, and VE-cadherin by targeting the MAPK signaling pathway.

Mig-7 enhances cell survival, migration, invasion, and tube formation via the MAPK pathway in U87MG cells. Next, we investigated the effects of Mig-7 on the survival, migration, invasion, and tube formation of U87MG cells. Upregulation of Mig-7 improved the survival, migration, invasion, and tube forming ability of U87MG cells; however,

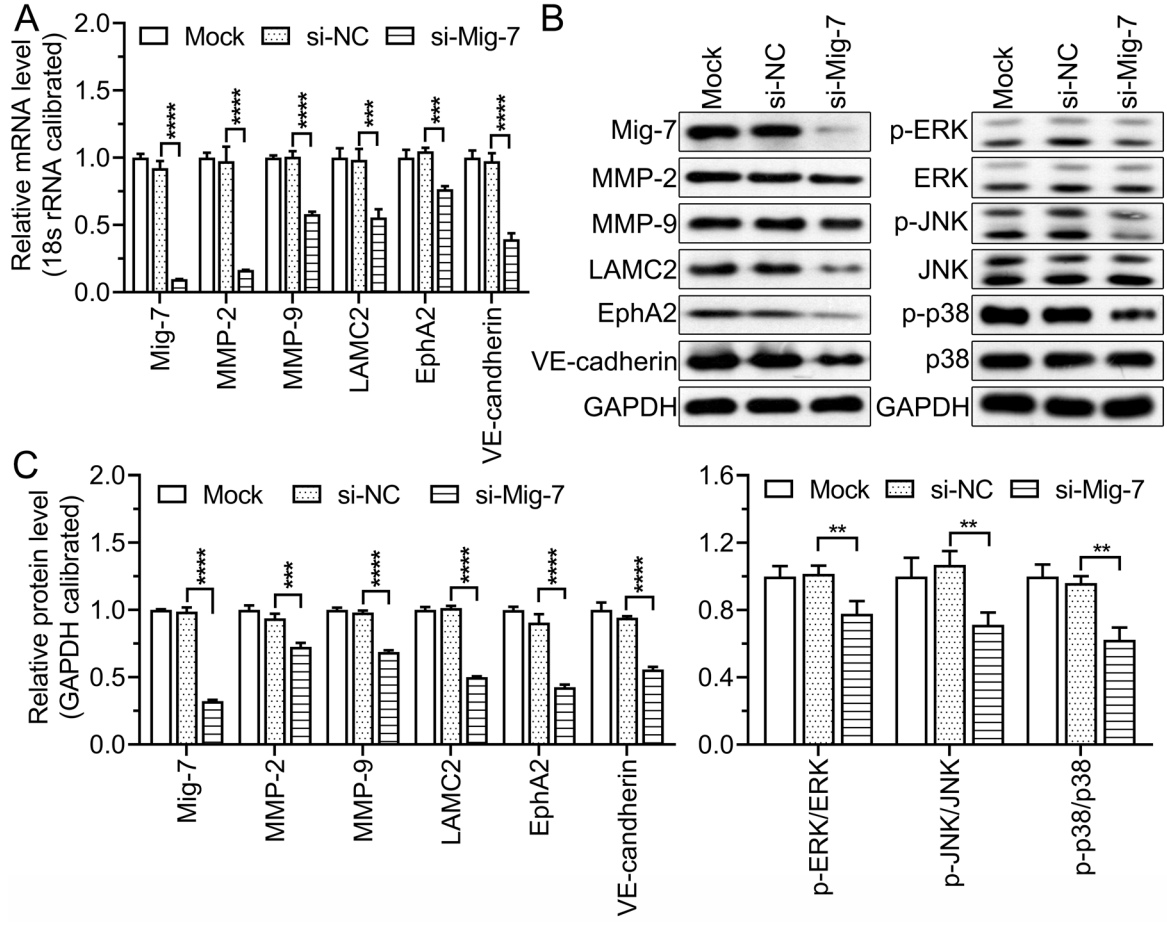

Figure 2. Knockdown of Mig-7 inhibits the expression of extracellular matrix-related molecules and the MAPK signaling pathway. A–C) The mRNA (A) and protein (B, C) levels of Mig-7, extracellular matrix- and MAPK pathway-related molecules were measured in U87MG cells by real-time PCR and western blotting after successful transfection of si-Mig-7. GAPDH was used as an internal control. These experiments were carried out independently three times (n=3). Statistical analysis was performed using one-way ANOVA (A, C). **p<0.01, ***p<0.001, ****p<0.0001. Abbreviation: Mig-7-migration-inducing gene-7

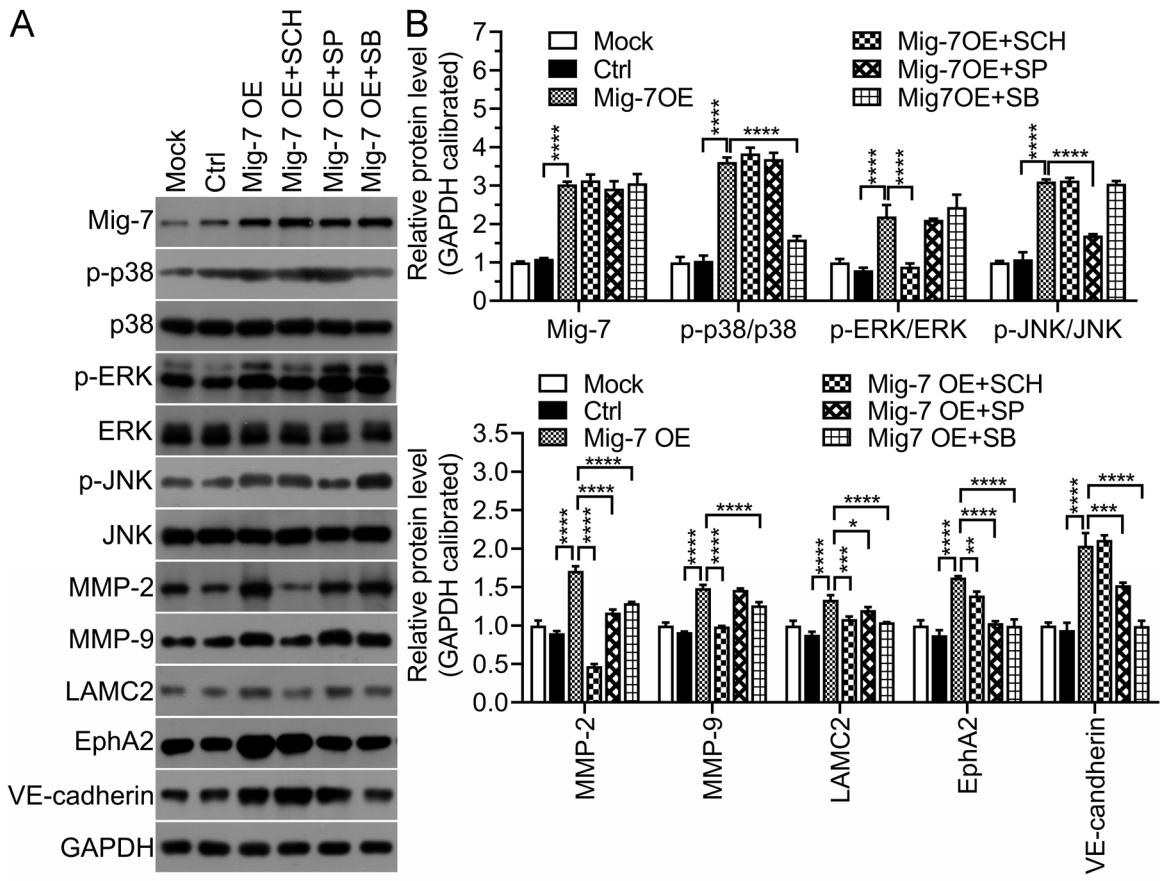

Figure 3. Mig-7 strengthens the expression levels of extracellular matrix-related molecules by activating the MAPK signaling pathway. A, B) Protein levels of extracellular matrix- and MAPK pathway-related molecules and Mig-7 were measured with western blotting after treatment of MAPK signaling pathway inhibitors into U87MG cells overexpressing Mig-7. GAPDH was used as an internal control. These experiments were carried out independently three times (n=3). Statistical analysis was performed using one-way ANOVA (B). *p<0.05, **p<0.01, ***p<0.001, ****p<0.0001. Abbreviation: Mig-7-migration-inducing gene-7

when treated with MAPK signaling pathway inhibitors (SP600125, SCH772984, or SB202190), the Mig-7-mediated effects of these cells were weakened (Figures 4A–4E, 5A, 5B) (multiple groups, one-way ANOVA; Figure 4A, $F_{5,30=}12.14$, p<0.0001; Figure 4C, $F_{5,12=}100.6$, p<0.0001; Figure 4E, $F_{5,12=}180.9$, p<0.0001; Figure 5B, $F_{5,12=}77.68$, p<0.0001).

Upregulation of Mig-7 promotes subcutaneous tumor formation in xenograft nude mice. To investigate the mechanism of action of Mig-7 *in vivo*, we performed animal experiments. In this study, all mice developed xenograft tumors at the injection site; nonetheless, tumor growth was observed to be significantly faster in the Mig-7 OE group than in the other two groups (Figure 6A) (multiple groups, one-way ANOVA, Figure 6A, 40 days: p=0.0005). Then, 40 days after injection the tumors were excised and weighed; the tumors of the Mig-7 OE group were significantly heavier and larger than those of the Ctrl and Mig-7 OE+MAPK inhibitors groups (Figures 6B, 6C) (multiple groups, one-way ANOVA, Figure 6C, tumor weight: $F_{2,15=}281.4$, p<0.0001). Further, when compared to tumors in the Ctrl group, expression levels of phosphor-JNK, phosphor-ERK, and phospho-p38 proteins were significantly higher in tumors excised from the Mig-7 OE group; additionally, this upregulated phosphorylation was reversed by MAPK inhibitors (Figures 6D, 6E) (multiple groups, one-way ANOVA, Figure 6E, phospho-p38/p38: $F_{5,12=}45.68$, p<0.0001, phospho-ERK/ERK: $F_{5,12=}19.24$, p=0.0006, phospho-JNK/JNK: $F_{5,12=}20.51$, p=0.0004). Immunohistochemical analysis with Ki-67 staining showed that the percentage of Ki-67-positive cells was significantly higher in the Mig-7 OE group than in the Ctrl group (Figures 6F, 6G) (multiple groups, one-way ANOVA, Figure 6G, Ki-67: $F_{2,15=}72.96$, p<0.0001). Therefore, upregulation of Mig-7 promoted the proliferation of glioma cells *in vivo*, probably by activating the MAPK pathways (phospho-JNK, phospho-ERK, and phospho-p38).

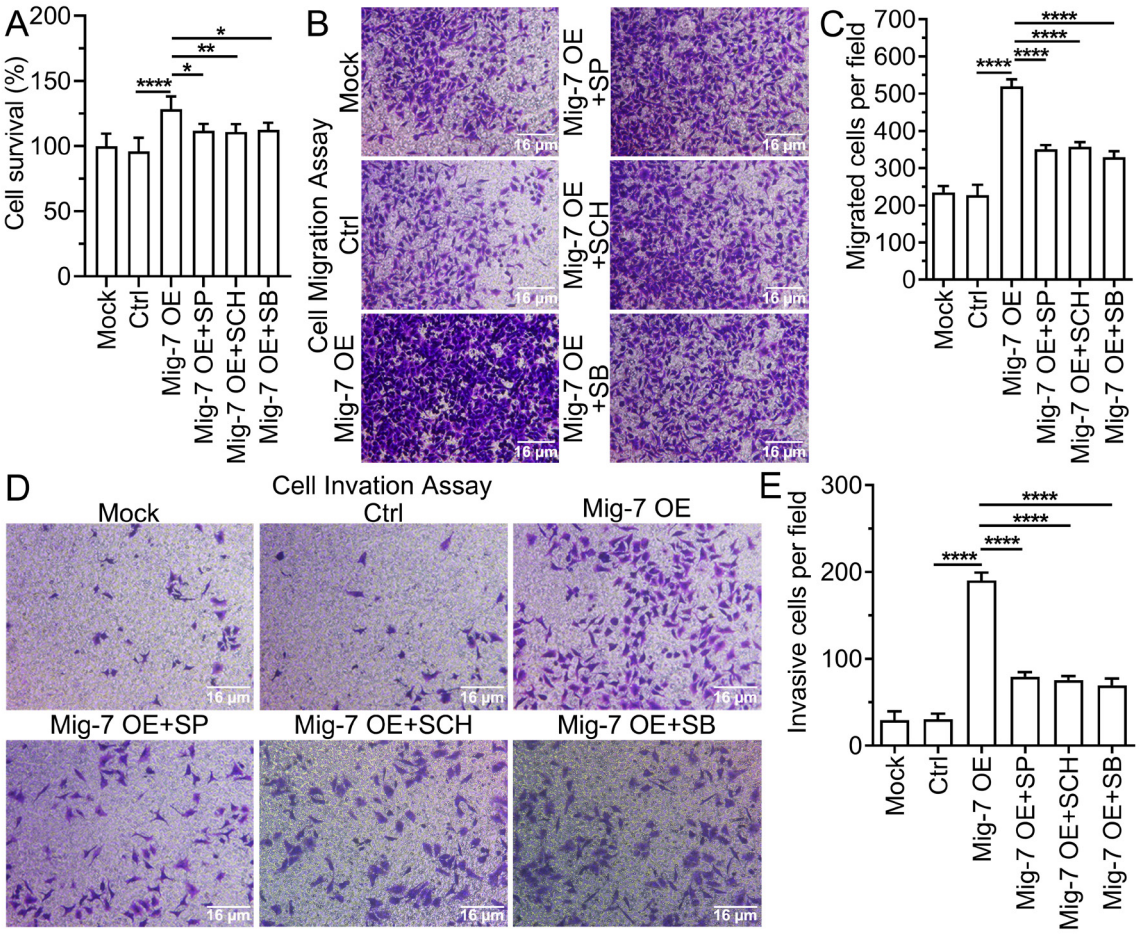

Figure 4. Mig-7 enhances cell survival, migration, and invasion via the MAPK pathway in U87MG cells. A) Cell survival was measured using MTT assay in U87MG cells after U87MG cells overexpressing Mig-7 were treated with MAPK signaling pathway inhibitors. B–E) Cell migration (B, C) and invasion (D, E) were detected after Mig-7-overexpressing U87MG cells were treated with MAPK signaling pathway inhibitors. These experiments were carried out independently three times (n=3). Statistical analysis was performed using one-way ANOVA (A, C, E). *p<0.05, **p<0.01, ***p<0.001, ****p<0.0001. Abbreviation: Mig-7-migration-inducing gene-7

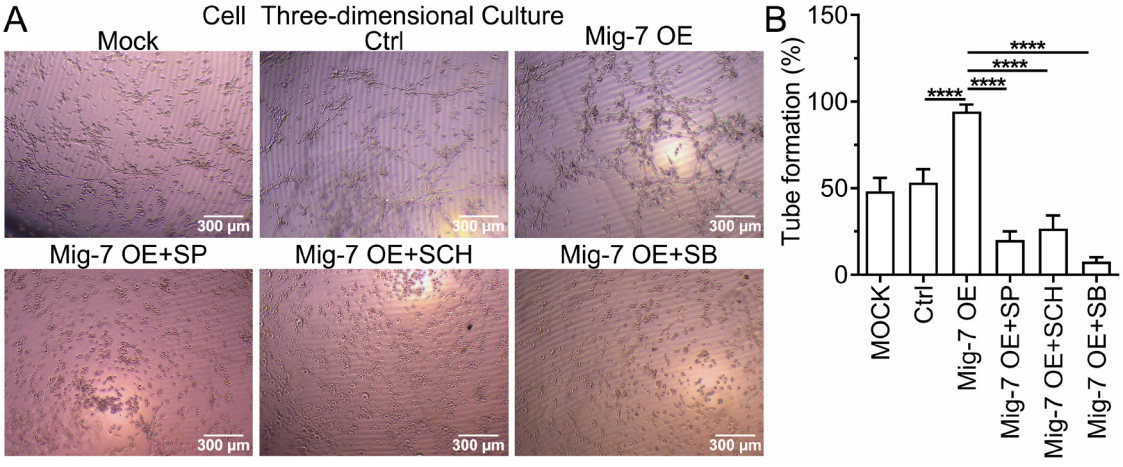

Figure 5. Mig-7 enhances tube formation via the MAPK pathway in U87MG cells. A, B) Tube formation was tested after Mig-7-overexpressing U87MG cells were treated with MAPK signaling pathway inhibitors. The experiment was carried out independently three times (n=3). Statistical analysis was performed using one-way ANOVA (B). ****p<0.0001. Abbreviation: Mig-7-migration-inducing gene-7

Discussion

Gliomas are primary malignant brain tumors [27]. The aggressiveness of this tumor is the main cause of its recurrence [28]. Therefore, exploring the molecular mechanisms that regulate glioma invasion will facilitate the development of novel drugs for the treatment of this disease.

It has been reported that Mig-7 is highly expressed in a variety of malignancies, including osteosarcoma, hepatocellular carcinoma, and ovarian cancer [8, 9]. Our results confirmed that Mig-7 mRNA and protein levels were higher in glioma tissues than in non-tumorigenic brain tissues, which corroborates with previous findings [12]. Additionally, Mig-7 mRNA and protein levels were also significantly upregulated in glioma cell lines (LN229, U87MG, and Hs 683 cell lines) compared to normal glial cell lines (HA1800). Moreover, Mig-7 can significantly affect tumor migration and invasion in glioma, hepatocellular carcinoma, and osteosarcoma [8, 9, 12]; further, Mig-7 is required for proliferation and invasion in ovarian cancer [9]. In this study, the upregulated expression of Mig-7 enhanced the migration and invasion of glioma cells. Moreover, overexpression of Mig-7 promoted the proliferation of glioma cells and tumor growth.

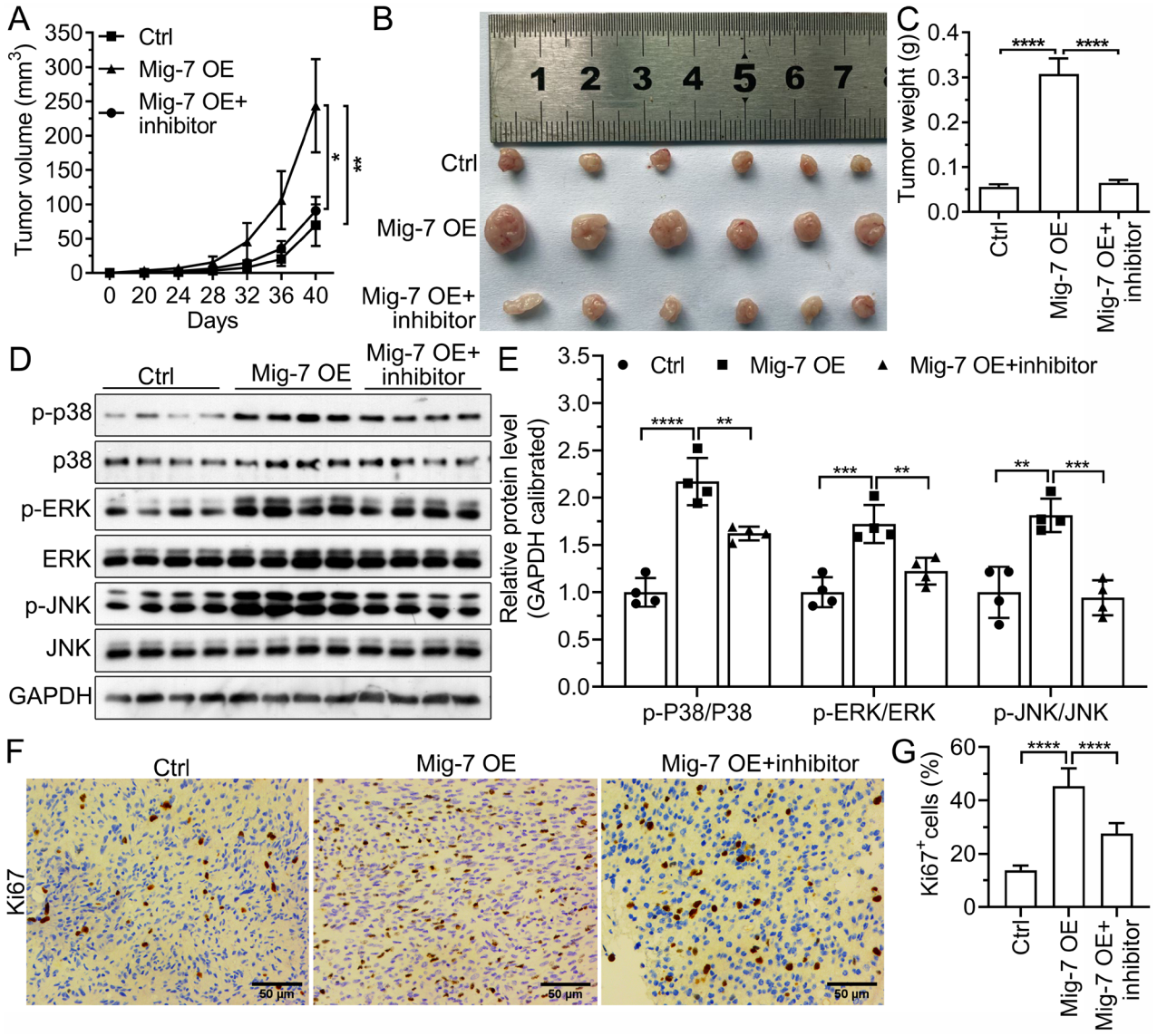

Figure 6. Upregulation of Mig-7 promotes subcutaneous tumor formation in nude mice. A) Tumor growth curves for each group (n=6). B) Resected tumors from nude mice 40 days after injection. C) Tumor weights were calculated after sacrificing nude mice 40 days after injection (n=6). D, E) Western blotting of MAPK signaling pathway-related protein expression (n=4). F) IHC analysis for detection of the proliferation marker Ki-67 (100× magnification). G) The percentage of Ki-67-positive cells was estimated under an optical microscope (n=6). Statistical analysis was performed using one-way ANOVA (A, C, E, G). *p<0.05, **p<0.01, ***p<0.001, ****p<0.0001. Abbreviation: Mig-7-migration-inducing gene-7

The MAPK pathway has been shown to be activated in gliomas, and the highly conserved MAPK pathway regulates various cellular functions, including proliferation, migration, and invasion [16, 29]. In addition, the PI3K/AKT pathway has been observed to play an important role in Mig-7 regulation of glioma invasiveness [12]; however, whether the MAPK pathway also plays an important role in Mig-7 regulation of glioma remains to be investigated. In this study, we determined that three MAPK signaling pathway inhibitors-JNK inhibitor SP600125, ERK inhibitor SCH772984, and p38 inhibitor SB202190-attenuated Mig-7-induced U87MG cell proliferation, migration, and invasion, as well as tumor growth. Additionally, MMP-2, MMP-9, LAMC2, EphA2, and VE-cadherin were determined to be involved in tumor cells invasion. Our results indicate that the protein levels of MMP-2, MMP-9, LAMC2, EphA2, and VE-cadherin increased by Mig-7 overexpression are reduced by MAPK signaling pathway inhibitors [30–34]. These results demonstrate that Mig-7 plays an important role in regulating glioma development via the MAPK pathway. Furthermore, three pathways, ERK, JNKs, and p38, are specifically involved in this process.

It has been reported that miR-520d-3p acts as a tumor suppressor by inhibiting vasculogenic mimicry (VM) formation by targeting Mig-7 [35]. Our previous findings showed a positive correlation between the level of Mig-7 protein expression and the amount of VM formation, which increased with the pathological grade of glioma [12]. It is evident that Mig-7 is closely associated with VM in glioma tissues. In addition, three-dimensional cell culture has been widely used as a method to detect the formation of VM *in vitro* [8, 9, 35], and was utilized in the present study. Our results demonstrated that overexpression of Mig-7 promoted tube formation, whereas the addition of MAPK signaling pathway inhibitors to these cells reversed the effect of Mig-7, suggesting that Mig-7 promotes tube formation by activating the MAPK signaling pathway in glioma cells. However, owing to the lack of VM-related detection in human glioma and mouse tumor tissues in this study, Mig-7 could not be verified to participate in glioma VM formation through the activation of the MAPK signaling pathway; this was considered to be one of the key limitations of this study.

Another limitation of this study is that we only investigated the effect of Mig-7 on the invasion ability of U87 MG cells at the cellular level without implementing corresponding animal experiments for *in vivo* verification.

In summary, Mig-7 enhances migration, invasion, cell viability, and tube formation of U87MG cells, as well as subcutaneous tumor formation in mice; specifically, these Mig-7-mediated effects occur via the activation of the MAPK signaling pathway. Overall, these results suggest that Mig-7 plays an important role in the occurrence and development of gliomas, suggesting that targeting Mig-7 for glioma treatment may be a promising therapeutic approach.

Acknowledgments: This research was supported by Startup Fund for Scientific Research, Fujian Medical University (Grant No. 2020QH1110), Natural Science Foundation of Fujian Province (Grant No. 2022J01788), and Medical Innovation project of Fujian Province (Grant No. 2021CXA025).

References

[1] BUSH NA, CHANG SM, BERGER MS. Current and future strategies for treatment of glioma. Neurosurg Rev 2017; 40: 1–14. https://doi.org/10.1007/s10143-016-0709-8

[2] OSTROM QT, GITTLEMAN H, TRUITT G, BOSCIA A, KRUCHKO C et al. CBTRUS Statistical Report: Primary Brain and Other Central Nervous System Tumors Diagnosed in the United States in 2011–2015. Neuro Oncol 2018; 20: iv1–iv86. https://doi.org/10.1093/neuonc/noy131

[3] QU S, QIU O, HUANG J, LIU J, WANG H. Upregulation of hsa-miR-196a-5p is associated with MIR196A2 methylation and affects the malignant biological behaviors of glioma. Genomics 2021; 113: 1001–1010. https://doi.org/10.1016/j.ygeno.2021.02.012

[4] CROUCH S, SPIDEL CS, LINDSEY JS. HGF and ligation of alphavbeta5 integrin induce a novel, cancer cell-specific gene expression required for cell scattering. Exp Cell Res 2004; 292: 274–287. https://doi.org/10.1016/j.yexcr.2003.09.016

[5] PETTY AP, GARMAN KL, WINN VD, SPIDEL CM, LINDSEY JS. Overexpression of carcinoma and embryonic cytotrophoblast cell-specific Mig-7 induces invasion and vessel-like structure formation. Am J Pathol 2007; 170: 1763–1780. https://doi.org/10.2353/ajpath.2007.060969

[6] PHILLIPS TM, LINDSEY JS. Carcinoma cell-specific Mig-7: a new potential marker for circulating and migrating cancer cells. Oncol Rep 2005; 13: 37–44.

[7] PETTY AP, WRIGHT SE, REWERS-FELKINS KA, YENDERROZOS MA, VORDERSTRASSE BA et al. Targeting migration inducting gene-7 inhibits carcinoma cell invasion, early primary tumor growth, and stimulates monocyte oncolytic activity. Mol Cancer Ther 2009; 8: 2412–2423. https://doi.org/10.1158/1535-7163.MCT-09-0186

[8] QU B, SHENG G, GUO L, YU F, CHEN G et al. MIG7 is involved in vasculogenic mimicry formation rendering invasion and metastasis in hepatocellular carcinoma. Oncol Rep 2018; 39: 679–686. https://doi.org/10.3892/or.2017.6138

[9] REN K, ZHANG J, GU X, WU S, SHI X et al. Migration-inducing gene-7 independently predicts poor prognosis of human osteosarcoma and is associated with vasculogenic mimicry. Exp Cell Res 2018; 369: 80–89. https://doi.org/10.1016/j.yexcr.2018.05.008

[10] CZEKIERDOWSKI A, CZEKIERDOWSKA S, STACHOWICZ N, ŁOZIŃSKI T, GURYNOWICZ G. Mig-7 expression and vasculogenic mimicry in malignant ovarian tumors. Ginekol Pol 2017; 88: 552–561. https://doi.org/10.5603/GP.a2017.0100

[11] FENG X, YAO J, GAO X, JING Y, KANG T et al. Multitargeting Peptide-Functionalized Nanoparticles Recognized Vasculogenic Mimicry, Tumor Neovasculature, and Glioma Cells for Enhanced Anti-glioma Therapy. ACS Appl Mater Interfaces 2015; 7: 27885–27899. https://doi.org/10.1021/acsami.5b09934

[12] PAN Z, ZHU Q, YOU W, SHEN C, HU W et al. Silencing of Mig-7 expression inhibits in-vitro invasiveness and vasculogenic mimicry of human glioma U87 Cells. Neuroreport 2019; 30: 1135–1142. https://doi.org/10.1097/WNR.0000000000001317

[13] TAPANEEYAKORN S, CHANTIMA W, THEPTHAI C, DHARAKUL T. Production, characterization, and in vitro effects of a novel monoclonal antibody against Mig-7. Biochem Biophys Res Commun 2016; 475: 149–153. https://doi.org/10.1016/j.bbrc.2016.05.062

[14] LIU X, GAO Q, ZHAO N, ZHANG X, CUI W et al. Sohlh1 suppresses glioblastoma cell proliferation, migration, and invasion by inhibition of Wnt/β-catenin signaling. Mol Carcinog 2018; 57: 494–502. https://doi.org/10.1002/mc.22774

[15] SUN S, KIANG KMY, HO ASW, LEE D, POON MW et al. Endoplasmic reticulum chaperone prolyl 4-hydroxylase, beta polypeptide (P4HB) promotes malignant phenotypes in glioma via MAPK signaling. Oncotarget 2017; 8: 71911–71923. https://doi.org/10.18632/oncotarget.18026

[16] WANG P, HAO X, LI X, YAN Y, TIAN W et al. Curcumin inhibits adverse psychological stress-induced proliferation and invasion of glioma cells via down-regulating the ERK/MAPK pathway. J Cell Mol Med 2021; 25: 7190–7203. https://doi.org/10.1111/jcmm.16749

[17] WEI J, LIU R, HU X, LIANG T, ZHOU Z et al. MAPK signaling pathway-targeted marine compounds in cancer therapy. J Cancer Res Clin Oncol 2021; 147: 3–22. https://doi.org/10.1007/s00432-020-03460-y

[18] PENG JM, CHEN YH, HUNG SW, CHIU CF, HO MY et al. Recombinant viral protein promotes apoptosis and suppresses invasion of ovarian adenocarcinoma cells by targeting α5β1 integrin to down-regulate Akt and MMP-2. Br J Pharmacol 2012; 165: 479–493. https://doi.org/10.1111/j.1476-5381.2011.01581.x

[19] LIVAK KJ, SCHMITTGEN TD. Analysis of relative gene expression data using real-time quantitative PCR and the 2(-Delta Delta C(T)) Method. Methods 2001; 25: 402–408. https://doi.org/10.1006/meth.2001.1262

[20] LI J, HU L, LIU Y, HUANG L, MU Y et al. DDX19A Senses Viral RNA and Mediates NLRP3-Dependent Inflammasome Activation. J Immunol 2015; 195: 5732–5749. https://doi.org/10.4049/jimmunol.1501606

[21] KIM SJ, CHOI HJ, JIN UH, LEE YC, KIM CH. Transcriptional regulation of the human Sia-alpha2,3-Gal-beta1,4-GlcNAc-R:alpha2,8-sialyltransferase (hST8Sia III) by retinoic acid in human glioblastoma tumor cell line. Biochim Biophys Acta 2006; 1759: 451–457. https://doi.org/10.1016/j.bbaexp.2006.09.003

[22] WANG C, ZHAO N, ZHENG Q, ZHANG D, LIU Y. BHLHE41 promotes U87 and U251 cell proliferation via ERK/cyclinD1 signaling pathway. Cancer Manag Res 2019; 11: 7657–7672. https://doi.org/10.2147/CMAR.S214697

[23] YANG XJ, CHEN GL, YU SC, XU C, XIN YH et al. TGF-β1 enhances tumor-induced angiogenesis via JNK pathway and macrophage infiltration in an improved zebrafish embryo/xenograft glioma model. Int Immunopharmacol 2013; 15: 191–198. https://doi.org/10.1016/j.intimp.2012.12.002

[24] TANG Y, YANG G, LI Y, WANG M, LI G et al. Protective effects of SP600125 on mice infected with H1N1 influenza A virus. Arch Virol 2021; 166: 2151–2158. https://doi.org/10.1007/s00705-021-05103-0

[25] YAN Z, OHUCHIDA K, FEI S, ZHENG B, GUAN W et al. Inhibition of ERK1/2 in cancer-associated pancreatic stellate cells suppresses cancer-stromal interaction and metastasis. J Exp Clin Cancer Res 2019; 38: 221. https://doi.org/10.1186/s13046-019-1226-8

[26] ZHANG G, JIN B, LI YP. C/EBPβ mediates tumour-induced ubiquitin ligase atrogin1/MAFbx upregulation and muscle wasting. EMBO J 2011; 30: 4323–4335. https://doi.org/10.1038/emboj.2011.292

[27] WANG G, WANG J, NIU C, ZHAO Y, WU P. Neutrophils: New Critical Regulators of Glioma. Front Immunol 2022; 13: 927233. https://doi.org/10.3389/fimmu.2022.927233

[28] ZHU Y, LIU X, ZHAO P, ZHAO H, GAO W et al. Celastrol Suppresses Glioma Vasculogenic Mimicry Formation and Angiogenesis by Blocking the PI3K/Akt/mTOR Signaling Pathway. Front Pharmacol 2020; 11: 25. https://doi.org/10.3389/fphar.2020.00025

[29] QIU D, ZHU Y, CONG Z. YAP Triggers Bladder Cancer Proliferation by Affecting the MAPK Pathway. Cancer Manag Res 2020; 12: 12205–12214. https://doi.org/10.2147/CMAR.S273442

[30] BARTOLOMÉ RA, TORRES S, ISERN DE VAL S, ESCUDERO-PANIAGUA B, CALVIÑO E et al. VE-cadherin RGD motifs promote metastasis and constitute a potential therapeutic target in melanoma and breast cancers. Oncotarget 2017; 8: 215–227. https://doi.org/10.18632/oncotarget.13832

[31] RATAJCZAK-WIELGOMAS K, KMIECIK A, DZIEGIEL P. Role of Periostin Expression in Non-Small Cell Lung Cancer: Periostin Silencing Inhibits the Migration and Invasion of Lung Cancer Cells via Regulation of MMP-2 Expression. Int J Mol Sci 2022; 23: 1240. https://doi.org/10.3390/ijms23031240

[32] NAZIR SU, KUMAR R, SINGH A, KHAN A, TANWAR P et al. Breast cancer invasion and progression by MMP-9 through Ets-1 transcription factor. Gene 2019; 711: 143952. https://doi.org/10.1016/j.gene.2019.143952

[33] WANG H, CAI J, DU S, WEI W, SHEN X. LAMC2 modulates the acidity of microenvironments to promote invasion and migration of pancreatic cancer cells via regulating AKT-dependent NHE1 activity. Exp Cell Res 2020; 391: 111984. https://doi.org/10.1016/j.yexcr.2020.111984

[34] WANG F, ZHANG H, CHENG Z. EPHA2 Promotes the Invasion and Migration of Human Tongue Squamous Cell Carcinoma Cal-27 Cells by Enhancing AKT/mTOR Signaling Pathway. Biomed Res Int 2021; 2021: 4219690. https://doi.org/10.1155/2021/4219690

[35] YAO N, ZHOU J, SONG J, JIANG Y, ZHANG J. miR-520d-3p/MIG-7 axis regulates vasculogenic mimicry formation and metastasis in osteosarcoma. Neoplasma 2022; 69: 764–775. https://doi.org/10.4149/neo_2022_211128N1683